Dyes and Pigments 80 (2009) 181–186

Contents lists available at ScienceDirect

Dyes and Pigments

journal homepage: www.elsevier.com/locate/dyepig

Crystal structures of C.I. Disperse Red 65 and C.I. Disperse Red 73

Ji-Eun Lee [a,b], Hyun Jee Kim [a], Mi Ran Han [c], Su Yeon Lee [c], Won Joo Jo [c], Shim Sung Lee [a,*], Jeong Sook Lee [c,**]

[a] Department of Chemistry (BK21) and Research Institute of Natural Science, Gyeongsang National University, Jinju 660-701, Republic of Korea
[b] Central Instrument Facility, Gyeongsang National University, Jinju 660-701, Republic of Korea
[c] Department of Clothing and Textiles, Engineering Research Institute, Gyeongsang National University, Jinju 660-701, Republic of Korea

ARTICLE INFO

Article history:
Received 23 May 2008
Received in revised form 3 July 2008
Accepted 5 July 2008
Available online 15 July 2008

Keywords:
Disperse dye
C.I. Disperse Red 65
C.I. Disperse Red 73
Crystal structure
H-bond
π–π Stacking interaction

ABSTRACT

Single crystals of C.I. Disperse Red 65 and C.I. Disperse Red 73 were grown from ethyl acetate and acetonitrile/toluene solutions, respectively, and their crystal structures were determined using single-crystal X-ray diffraction analysis. In each dye molecule, the aminoazobenzene framework is almost planar due to intramolecular H-bonding. In the case of C.I. Disperse Red 65, intermolecular associations occur by π–π stacking and intermolecular H-bonding, resulting in a herringbone-type arrangement; for C.I. Disperse Red 73, toluene molecules stabilize the crystal structure via π–π stacking.

1. Introduction

Due to their central role in the dyeing polyester fibers and high-tech applications, disperse dyes have attracted the attention of researchers [1]. The structural investigation of disperse dyes in solid state has been emphasized because the absorption and dyeing behaviors such as dye uptake by the polyester fiber are dependent not only on the conformation of the solid dye but also on the interactions between fiber surface and dye in molecular level [2–10]. The technical performance of the disperse dyes is related with their morphology, particle size and conformation in crystalline state [11]. Furthermore, the demand for the development of new functional dyes also requires additional information including the structural conformations of already existing dyestuff in molecular level. As a part of research program for the structure/function relationships of the dye molecules, we have reported the crystal structures of several types of disperse dyes such as monoazo [12–14], methine [15] and anthraquinone [16] dyes. In particular, disperse azo dyes have been continuously used in the paper, foodstuffs and leather as well as textile industry [1]. Following our interest into the structural characteristics of such disperse dye molecules, we describe here the crystal structures of two commercially important azo-type red dyes, C.I. Disperse Red 65 (C.I. number 11228) and Red 73 (C.I. number 11116).

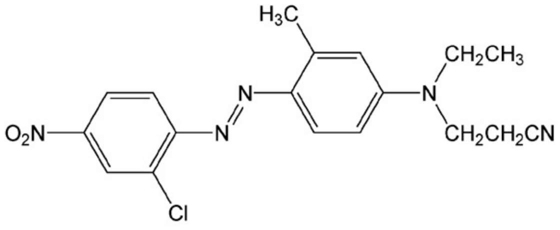

C. I. Disperse Red 65

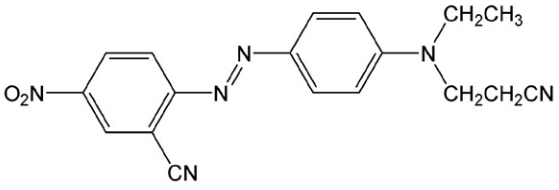

C. I. Disperse Red 73

---

* Corresponding author. Tel.: +82 55 751 6021.
** Corresponding author. Tel.: +82 55 751 5985.
E-mail addresses: sslee@gnu.ac.kr (S.S. Lee), jslee@gnu.ac.kr (J.S. Lee).

0143-7208/$ – see front matter © 2008 Elsevier Ltd. All rights reserved.
doi:10.1016/j.dyepig.2008.07.001

Table 1
Crystallographic data for C.I. Disperse Red 65 and C.I. Disperse Red 73

	Red 65	Red 73
Empirical formula	$C_{18}H_{18}ClN_5O_2$	$C_{25}H_{24}N_6O_2$
Formula weight	371.82	440.50
Temperature (K)	173(2)	173(2)
Wavelength (Å)	0.71073	0.71073
Crystal system	Monoclinic	Monoclinic
Space group	$C2/c$	$C2/c$
a (Å)	30.412(5)	35.363(4)
b (Å)	7.8362(13)	6.9778(8)
c (Å)	15.399(2)	20.250(2)
β (°)	104.067(3)	114.078(2)
Volume (Å^3)	3559.7(10)	4561.9(9)
Z	8	8
D_{calc} (g/cm^3)	1.388	1.283
μ (mm^{-1})	0.238	0.085
F(000)	1552	1856
Crystal dimensions (mm)	0.30 × 0.20 × 0.02	0.50 × 0.40 × 0.10
Color of crystal	Red	Red
Shape of crystal	Plate	Block
$2\theta_{max}$ (°)	54.00	54.00
No. of reflections measured	10448	13424
No. of reflections observed [$I > 2\sigma(I)$]	3861	4921
No. of variables	235	315
R	0.0625	0.0975
R_w	0.1253	0.2744
Largest diff. peak and hole (e Å^{-3})	0.289 and −0.317	0.965 and −0.517
Maximum shift in final cycles	<0.001	<0.001

Table 3
Selected bond lengths (Å) and bond angles (°) for C.I. Disperse Red 73

O(1)–N(1)	1.219(4)	O(2)–N(1)	1.215(4)
N(1)–C(2)	1.472(4)	N(6)–C(7)	1.125(5)
N(2)–N(3)	1.272(4)	N(2)–C(5)	1.414(4)
N(3)–C(8)	1.387(4)	N(4)–C(11)	1.357(5)
N(4)–C(16)	1.443(6)	N(4)–C(14)	1.464(5)
N(5)–C(18)	1.152(18)	N(5′)–C(18′)	1.126(9)
C(1)–C(2)	1.375(5)	C(1)–C(6)	1.400(5)
C(2)–C(3)	1.386(5)	C(3)–C(4)	1.379(5)
C(4)–C(5)	1.391(5)	C(5)–C(6)	1.402(5)
C(6)–C(7)	1.453(5)	C(8)–C(9)	1.402(5)
C(8)–C(13)	1.405(5)	C(9)–C(10)	1.373(5)
C(10)–C(11)	1.409(5)	C(11)–C(12)	1.425(5)
C(12)–C(13)	1.369(5)	C(14)–C(15)	1.503(7)
C(16)–C(17)	1.489(7)	C(16)–C(17′)	1.498(7)
C(17)–C(18)	1.480(18)	C(17′)–C(18′)	1.534(10)
C(19)–C(20)	1.546(10)	C(20)–C(22)	1.379(7)
C(20)–C(21)	1.384(6)		
O(2)–N(1)–O(1)	123.4(3)	O(2)–N(1)–C(2)	118.5(3)
O(1)–N(1)–C(2)	118.1(3)	N(3)–N(2)–C(5)	111.9(3)
N(2)–N(3)–C(8)	116.4(3)	C(11)–N(4)–C(16)	123.1(3)
C(11)–N(4)–C(14)	121.1(3)	C(16)–N(4)–C(14)	115.8(3)
C(2)–C(1)–C(6)	117.1(3)	C(1)–C(2)–C(3)	123.4(3)
C(1)–C(2)–N(1)	118.6(3)	C(3)–C(2)–N(1)	118.0(3)
C(4)–C(3)–C(2)	118.4(3)	C(3)–C(4)–C(5)	121.0(3)
C(4)–C(5)–C(6)	118.7(3)	C(4)–C(5)–N(2)	124.8(3)
C(6)–C(5)–N(2)	116.5(3)	C(1)–C(6)–C(5)	121.3(3)
C(1)–C(6)–C(7)	118.7(3)	C(5)–C(6)–C(7)	120.0(3)
N(6)–C(7)–C(6)	177.3(4)	N(3)–C(8)–C(9)	115.8(3)
N(3)–C(8)–C(13)	126.2(3)	C(9)–C(8)–C(13)	118.0(3)
C(10)–C(9)–C(8)	121.6(3)	C(9)–C(10)–C(11)	121.0(3)
N(4)–C(11)–C(10)	121.0(3)	N(4)–C(11)–C(12)	121.8(3)
C(10)–C(11)–C(12)	117.2(3)	C(13)–C(12)–C(11)	121.3(3)
C(12)–C(13)–C(8)	121.0(3)	N(4)–C(14)–C(15)	113.5(4)
N(4)–C(16)–C(17)	112.1(6)	N(4)–C(16)–C(17′)	145.6(12)
C(17)–C(16)–C(17′)	34.8(12)	C(18)–C(17)–C(16)	110.8(12)
N(5)–C(18)–C(17)	177(2)	C(16)–C(17′)–C(18′)	103.3(13)
N(5′)–C(18′)–C(17′)	152(3)		

2. Experimental

The C.I. Disperse Red 65 and Red 73 purchased from Longsheng Co. were extracted with dichloromethane to separate the colorant from diluents. The single crystals suitable for the X-ray analysis were obtained by slow evaporation of ethyl acetate (Red 65) and acetonitrile/toluene (Red 73) solution of the respective purified dyes. The suitable each crystal was mounted on a Bruker SMART diffractometer equipped with a graphite monochromated Mo Kα ($\lambda = 0.71073$ Å) radiation source and a CCD detector and 45 frames of two-dimensional diffraction images were collected and processed to deduce the cell parameters and orientation matrix. A total 1271 and frames of two-dimensional diffraction images were collected, each of which was measured. The frame data were processed to give structure factors using the program SAINT [17]. The intensity data were corrected for Lorentz and polarization effects. The structures were solved by a combination of direct and difference Fourier methods provided by the program package SHELXTL [18] and refined a full matrix least square against F^2 for all data. All non-hydrogen atoms were refined anisotropically. In Red 73, the toluene molecules are disordered by crystallographic symmetry over two sites with occupancy of 50%. The –CH_2CN terminal in the same molecule is also disordered over two sites in a 60:40 ratio. Due to these disorder and large thermal vibrations, the R value and displacement parameters are larger than desired. All hydrogen atoms were included in calculated positions with isotropic thermal parameters 1.2 times those of attached atoms. Crystallographic data are summarized in Table 1. CCDC reference numbers 687189 (Red 65) and 687190 (Red 73).

Table 2
Selected bond lengths (Å) and bond angles (°) for C.I. Disperse Red 65

Cl(1)–C(3)	1.740(4)	O(1)–N(1)	1.231(4)
O(2)–N(1)	1.225(4)	N(1)–C(1)	1.471(5)
N(2)–N(3)	1.276(4)	N(2)–C(4)	1.415(5)
N(3)–C(8)	1.394(5)	N(4)–C(11)	1.371(5)
N(4)–C(17)	1.458(5)	N(4)–C(15)	1.460(5)
N(5)–C(19)	1.138(5)	C(1)–C(2)	1.369(5)
C(1)–C(6)	1.382(6)	C(2)–C(3)	1.379(5)
C(3)–C(4)	1.397(5)	C(4)–C(5)	1.396(5)
C(5)–C(6)	1.380(5)	C(8)–C(9)	1.406(5)
C(8)–C(13)	1.417(5)	C(9)–C(10)	1.358(5)
C(10)–C(11)	1.417(5)	C(11)–C(12)	1.412(5)
C(12)–C(13)	1.386(5)	C(13)–C(14)	1.498(5)
C(15)–C(16)	1.525(6)	C(17)–C(18)	1.539(5)
C(18)–C(19)	1.468(6)		
O(2)–N(1)–O(1)	123.0(4)	O(2)–N(1)–C(1)	118.6(4)
O(1)–N(1)–C(1)	118.4(4)	N(3)–N(2)–C(4)	113.5(3)
N(2)–N(3)–C(8)	113.3(3)	C(11)–N(4)–C(17)	122.8(3)
C(11)–N(4)–C(15)	121.7(3)	C(17)–N(4)–C(15)	115.3(3)
C(2)–C(1)–C(6)	123.1(4)	C(2)–C(1)–N(1)	117.9(4)
C(6)–C(1)–N(1)	119.0(4)	C(1)–C(2)–C(3)	118.0(4)
C(2)–C(3)–C(4)	121.4(4)	C(2)–C(3)–Cl(1)	118.5(3)
C(4)–C(3)–Cl(1)	120.2(3)	C(5)–C(4)–C(3)	118.4(4)
C(5)–C(4)–N(2)	125.2(4)	C(3)–C(4)–N(2)	116.4(3)
C(6)–C(5)–C(4)	121.0(4)	C(5)–C(6)–C(1)	118.0(4)
N(3)-C(8)-C(9)	124.1(4)	N(3)-C(8)-C(13)	117.3(3)
C(9)–C(8)–C(13)	118.6(4)	C(10)–C(9)–C(8)	122.1(4)
C(9)–C(10)–C(11)	120.7(4)	N(4)–C(11)–C(12)	122.7(4)
N(4)–C(11)–C(10)	120.1(4)	C(12)–C(11)–C(10)	117.2(4)
C(13)–C(12)–C(11)	122.6(4)	C(12)–C(13)–C(8)	118.8(4)
C(12)–C(13)–C(14)	120.1(4)	C(8)–C(13)–C(14)	121.1(4)
N(4)–C(15)–C(16)	112.0(4)	N(4)–C(17)–C(18)	111.3(3)
C(19)–C(18)–C(17)	111.1(4)	N(5)–C(19)–C(18)	178.3(5)

3. Results and discussion

The absence of the single-crystal structural data for the title compounds may be due, in part, to the difficulty in growing crystals acceptable for X-ray diffraction analysis. Our attempts to

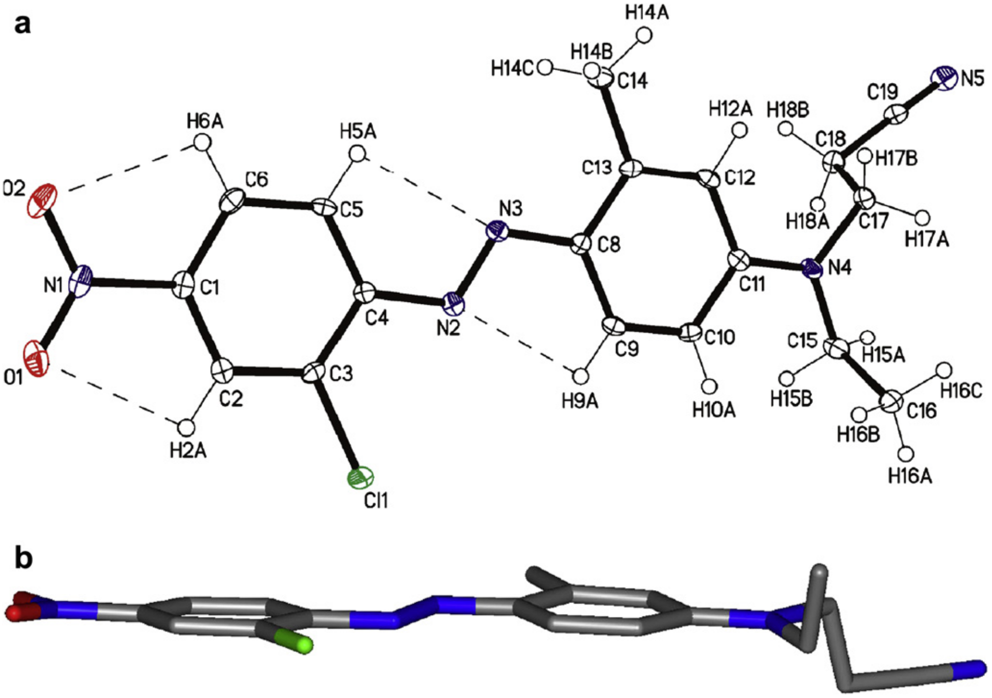

Fig. 1. X-ray crystal structure of C.I. Disperse Red 65: (a) top view with intramolecular H-bonds (dashed lines) and (b) side view showing the planarity.

grow the single crystals from organic solvents such as methanol, ethanol, dichoromethane and acetonitrile always afforded amorphous solid or needle-shape crystals, none of which diffracted well enough got solving the crystal structure. Acceptable red crystals suitable for X-ray analysis were produced by slow evaporation of the ethyl acetate (Red 65) and acetonitrile/toluene (Red 73) solutions of the purified dyes after several weeks at the room temperature, respectively. The both crystals used exist in the monoclinic space group *C*2/*c*. The bond lengths and angles are reported in Tables 2 and 3. The crystal structures are given in Figs. 1 and 2.

The aminoazobenzene framework of each dye is essentially planar with dihedral angles of 3.45(2)° for Red 65 and 2.44(1)° for Red 73 between two phenyl rings (Figs. 1b and 2b). In Red 65, the anti-arrangement of Cl atom and methyl group is due to the repulsive force between two units. Notably, overall structures of the dye molecules are also planar. The unsubstituted aminoazobenzene moiety in some other derivatives often shows non-planarity with much larger dihedral angles (21.2–46.5°) [19–21]. So, the planar conformations for both molecules are, at least in part, due to the stabilization by the intramolecular H-bonds such as C–H···O and C–H···N types (dashed lines in Figs. 1a and 2a), which have bond

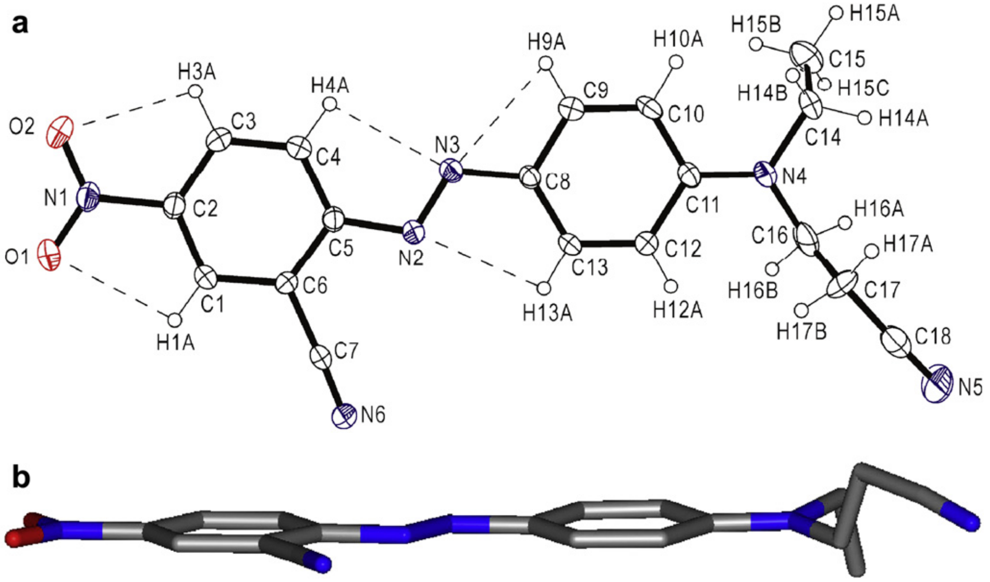

Fig. 2. X-ray crystal structure of C.I. Disperse Red 73: (a) top view with intramolecular H-bonds (dashed lines) and (b) side view showing the planarity.

Table 4
Intra- and intermolecular H-bonds geometry (Å, °) for C.I. Disperse Red 65

D–H···A	D–H	H···A	D···A	D–H···A
C2–H2A···O1	0.95	2.40	2.701(5)	61.6
C5–H5A···N3	0.95	2.47	2.730(5)	64.2
C6–H6A···O2	0.95	2.45	2.732(5)	62.8
C9–H9A···N2	0.95	2.41	2.688(5)	63.0
C15–H15B^{iii}···N5	0.95	2.62	3.478(6)	145.7
C15–H15A^{iii}···O1^{i}	0.95	2.76	3.594(5)	142.8
C15–H15A^{iii}···O2^{i}	0.95	2.63	3.599(5)	166.2

Table 5
Intra- and intermolecular H-bonds geometry (Å, °) for C.I. Disperse Red 73

D–H···A	D–H	H···A	D···A	D–H···A
C1–H1A···O1	0.93	2.43	2.707(4)	62.9
C3–H3A···O2	0.93	2.42	2.706(5)	62.1
C4–H4A···N3	0.93	2.41	2.681(5)	63.5
C9–H9A···N3	0.93	2.50	2.362(4)	87.3
C13–H13A···N2	0.93	2.54	2.783(4)	65.6
C1–H1A···N5^{i}	0.93	2.66	3.448(11)	142.9
C12–H12A···N6^{i}	0.93	2.75	3.681(5)	174.5

length ca. 2.4–2.8 Å (Tables 4 and 5). In both cases, for example, the 4-nitro groups are almost coplanar with the phenyl ring (C1–C6) and as indicated by the dihedral angle of 3.52(6)° for Red 65 and 1.25(1)° for Red 73, which are also due to the H-bonds between nitro O atoms and adjacent aromatic CH atoms. Two *N*-alkyl chains in each molecule tend to be separated as far apart as possible with one alkyl chain being above the aminobenzene plane and another one below both it.

Although both compounds form networks in packing, there are differences in the way the H-bonds and aromatic π–π stacking interactions are involved. In the packing of both structures, they include the head-to-tail mode molecular stacking (Figs. 3a and 4a). In such a way they form the stacked array with interlayer associations by means of the aromatic π–π stacking interaction with distances of 3.8–4.0 Å. In addition, the intermolecular hydrogen bonds, which stabilized the molecular packing are also observed (Tables 4 and 5). The Red 65 molecules show the characteristic herringbone-type packing arrangement in which the offset-face-to-face π–π stacking (dotted lines) and intermolecular H-bonds (dashed lines) are responsible for this orientation (Fig. 3). Notably, in Red 73, disordered toluene molecules exist in the space between individual pairs of dye molecules forming edge-to-face type π–π interactions (Fig. 4). The single crystals of Red 73 slowly became cloudy loosing the solvent molecules at room temperature, indicating that the solvent toluene molecules play a key role in the preparation of single crystals for Red 73.

In summary, the single crystals of C.I. Disperse Red 65 and Disperse Red 73 were grown and their crystal structures were characterized by X-ray analysis. In view of the single molecule for both molecules, the planar structures are stabilized by the multiple intramolecular H-bonds bonds in each case. In case of Red 65, intermolecular associations occur by further π–π stacking and intermolecular H-bonds show the herringbone-type packing arrangement. In case of Red 73, toluene molecules stabilize the crystal packing via π–π stacking. These structural aspects which show diverse types of weak inter- and intramolecular interactions

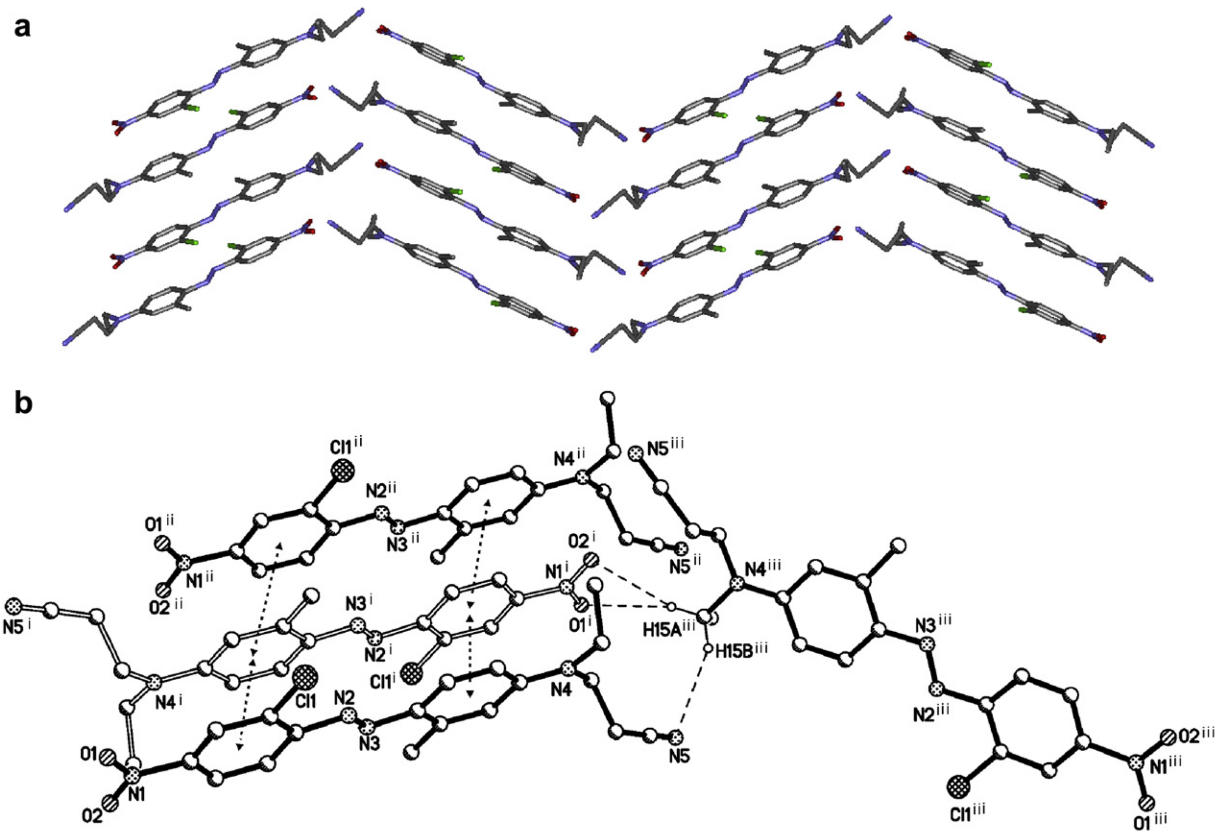

Fig. 3. (a) Herringbone-type packing arrangement and (b) intermolecular interactions by H-bonds (dashed lines) and π–π stacking (dotted lines) for Disperse Red 65. [symmetry codes: (i) $-x+1, y-1, -z+1$; (ii) $x, y+1, z$; (iii) $-x+1/2, y+1/2, -z+1/2$].

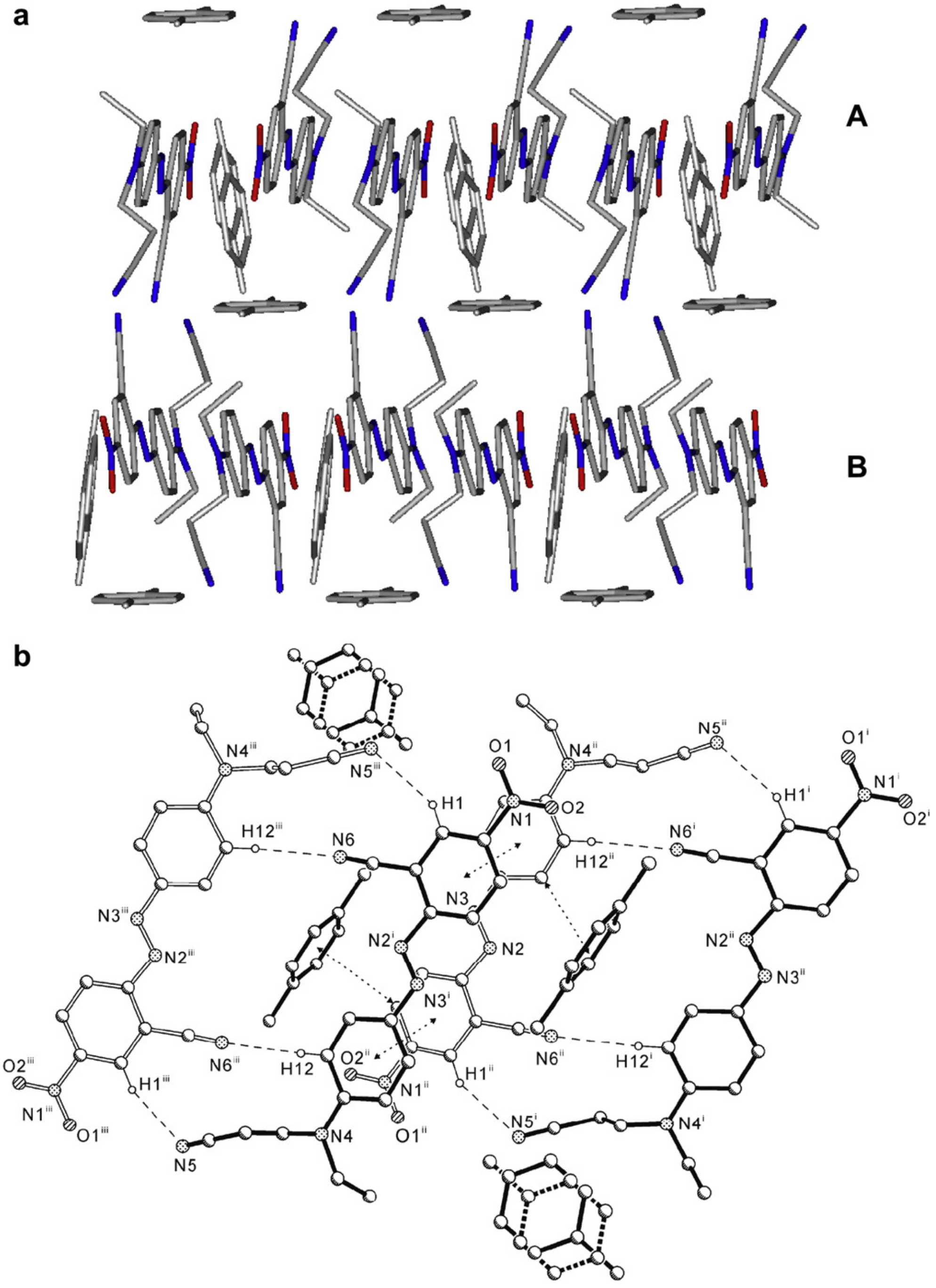

Fig. 4. (a) Bookshelf-type packing arrangement and (b) intermolecular interactions by H-bonds (dashed lines) and π–π stacking (dotted arrows) for Disperse Red 73 with disordered toluene molecules. [symmetry codes: (i) $-x+1$, $-y+3$, $-z+1$; (ii) $-x+1$, y, $z-1$; (iii) x, $-y+3$, $z+1/2$].

may be viewed as characteristic features of the substituted aminoazobenzene-type dyes.

Acknowledgement

The support of the Chemistry Research and Scholarship Foundation at GNU is gratefully acknowledged.

References

[1] Dawson JF. J Soc Dyers Color 1983;99:183.
[2] Annen O, Egli R, Hasler R, Henzo B, Jakob H, Matzinger P. Rev Prog Color 1987;17:72.
[3] Leadbetter PW, Leaver AT. Rev Prog Color 1989;19:33.
[4] McIntosh SA, Freeman HS. Tex Res J 1989;59:389.
[5] McIntosh SA, Freeman HS, Singh P. Dyes Pigments 1992;20:147.
[6] Freeman HS, Posey Jr JC. Dyes Pigments 1992;20:147.
[7] Freeman HS, Posey Jr JC, Singh P. Dyes Pigments 1992;20:279.
[8] Freeman HS, McIntosh SA, Singh P. Dyes Pigments 1997;35:11.
[9] Freeman HS, McIntosh SA, Singh P. Dyes Pigments 1997;35:149.
[10] You X-L, Lu C-R, Huang Z-L, Zhang D-C. Dyes Pigments 2004;63:217.
[11] McGeorge G, Harris RK, Batsanov AS, Churakov AV, Chippendale AM, Bullock JF, et al. J Phys Chem A 1998;102:3505.
[12] Park K-M, Yoon I, Lee SS, Choi G, Lee JS. Dyes Pigments 2002;54:155.
[13] Seo J, Jo WJ, Choi G, Park K-M, Lee SS, Lee JS. Dyes Pigments 2007;72:327.
[14] Seo J, Jo WJ, Choi G, Han MR, Lee SY, Lee SS, et al. Dyes Pigments 2008;76:530.
[15] Yoon I, Park K-M, Lee SS, Choi G, Lee JS. Anal Sci 2001;17:1355.
[16] Park K-M, Yoon I, Lee SS, Choi G, Lee JS. Anal Sci 2003;19:1219.

[17] Bruker. Area detector control and integration software, Version 6.22. In: SAMRT and SAINT. Madison, Wisconsin (USA): Bruker Anaytical X-ray Instruments Inc.; 2001.
[18] Bruker. Structure determination programs, Version 6.10. In: SHELXTL. Madison, Wisconsin (USA): Bruker Analytical X-ray Instruments Inc.; 2000.
[19] Lee HG, Lee J-E, Choi KS. Inorg Chem Commun 2006;9:582.
[20] Centore R, Carella A, Pugliese A, Sirigu A, Tuzi A. Acta Crystallogr 2006;C62:o531.
[21] Lacroix PG, Malfant I, Iftime G, Razus AC, Nakatani K, Delaire JA. Chem Eur J 2000;6:2599.